Stochastic Tapped Delay Line Based One-Sided Beamformed Channel Impulse Response Models of LoS and Reflected Waves at 62.5 GHZ in A Conference Room Environment

Lawrence Materum
Electronics and Communications Engineering Department,
De La Salle University, Manila, Philippines.
materuml@dlsu.edu.ph

***Abstract*—Novel statistical channel models based on tapped-delay lines are proposed for the evaluation of indoor millimeter-wave wireless communication systems. The considered frequency bands for its application are around the 62.5-GHz region for wireless personal area networks. The channel characterization was carried out inside a conference room environment with fixed communication links. The proposed models acquire the significant paths in the propagation channel that are necessary to achieve high gigabit-per-second throughput by using directive (high-gain) antennas that emulate the radiation pattern of beamforming antenna systems. The anticipated application is for simulating wireless systems inside conference rooms under line-of-sight (LoS) conditions, and under non-LoS conditions wherein the transceiver seeks the candidate signal path among the reflected waves and then switches to the best signal-to-noise ratio path so that a high-rate link could continue. As indicated by the modeling results, only several paths are useful for very high speed communication rates. These paths and the effects they bring to the receiver, like delay spread, are taken into account by the proposed millimeter-wave channel models.**

***Index Terms*—Multipath Channels; Channel Models; Millimeter Wave Propagation; Beamforming; Directive Antennas.**

I. INTRODUCTION

The global availability of the 57 GHz to 66 GHz millimeter-wave (mmWave) band for wireless personal area networks (WPANs) has spurred interest in achieving gigabit per second (Gbps) throughput envisioned initially by the IEEE 802.15.3c and IEEE 802.11ad Task Groups, which have released the first over-Gbps WPAN standard [1] and wireless local area network (WLAN) standard [2] for indoor mmWave communications, respectively. One of the limiting factors in realizing such throughput is related to the understanding of the mmWave channel in indoor environments. As dictated by physics, the channel contains links that increase in attenuation as the propagation path distance extends. This attenuation is more severe at mmWave bands due to atmospheric absorption [3] and high frequency according to Friss transmission [4]. This means only certain paths would be useful in establishing communications. Contrasting this with ultra-high frequency (UHF) propagation channels used by cellular terminals, the establishment of links could readily be achieved around the terminal. Since majority of current channel models have been made for UHF propagation, the methodology employed in characterizing the mmWave propagation channel has been almost similar, i.e. all the paths around the terminal side are taken into account. From a user point of view, it is desirable to have low-cost portable terminals. This implies that future terminals supporting indoor mmWave communications must be able to make the radio system as simple as possible at the least cost. One of the questions then that this paper seeks to answer is what channel model would be able to capture such views? An oversight then of previous mmWave channel modeling efforts [5], [6] is the determination of the useful components of the propagation channel. Such components could be seen as paths that can be switched to with beamforming antenna systems. The difference then from IEEE 802.15.3c and IEEE 802.11ad channel models from those proposed here is the modeling of only those paths that are useful for establishing high throughput communications. The proposed channel models are for mmWave beamforming systems employed in conference rooms.

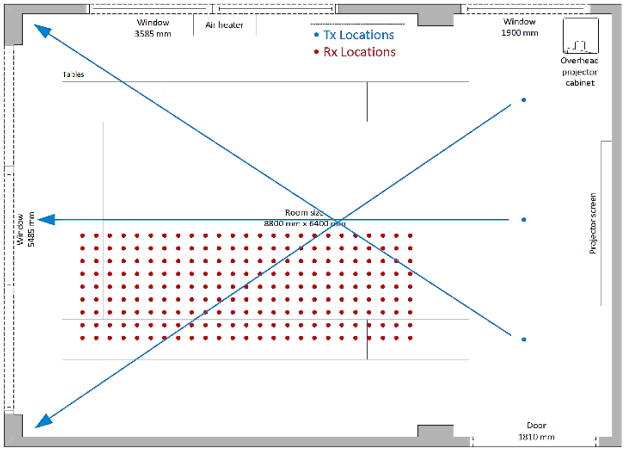

Figure 1: Conference room layout showing the 3 Tx and 225 Rx locations. The pointing direction (indicated by an arrow) of each Tx antenna was chosen in order to maximize the coverage in the room. Each Tx antenna was used one at a time. The Tx and Rx antennas are mounted at 1-m height from the floor. The size of the room is 8.8 m × 6.4 m

Ray tracing was done in a conference room, from which the statistical parameters of the channel were extracted, the details of which are discussed in Section II. The tapped-delay line (TDL) model is described and the specific models are

validated in Section III in which the models were found to be close to the simulation data. Lastly, concluding remarks are given in Section IV.

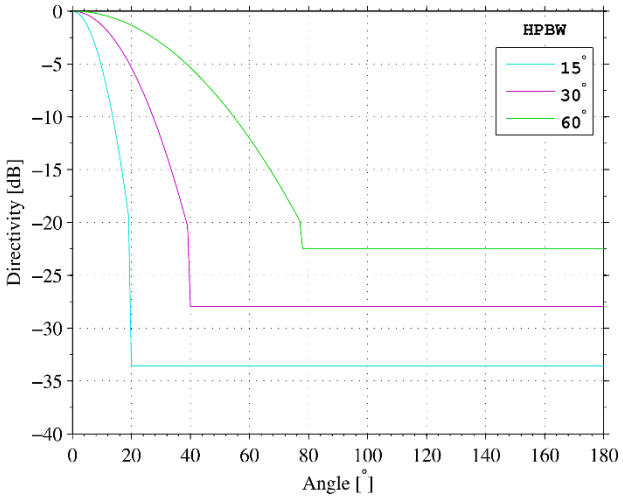

Figure 2: IEEE 802.11ad and IEEE 802.15.3c reference antenna patterns [8] that were utilized

Table 1
Beam Levels of the Antenna Models [8]

HPBW [°]	Max. gain [dBi]	Sidelobe down [dB]
60	10.21	22.49
30	15.93	27.93
15	21.88	33.59

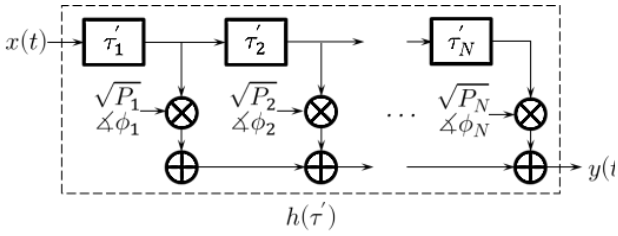

Figure 3: A tapped-delay line (TDL) filter with N taps. $\sqrt{\mathrm{P_n}}$ amplitude and ϕ_n phase indicate the weight at the nth tap with τ_n' delay. The output is obtained as $y(t) = \int_{-\infty}^{\infty} x(t-\tau')h(\tau')\mathrm{d}\tau'$

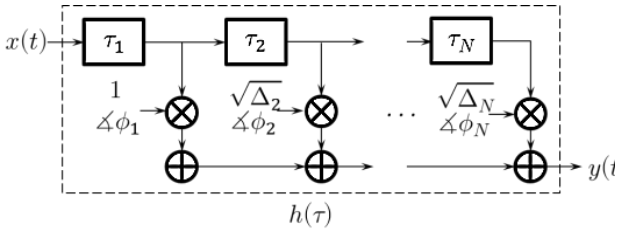

Figure 4: Modified tapped-delay line model for the channel impulse response. Tap amplitudes are normalized with respect to the highest one, which is placed at the first tap. $\Delta_2$onwards represent the power level difference from Δ_1 (= 0 dB), and τ_n represents the excess delay

II. Ray Tracing in a Conference Room

The indoor environment considered is a conference room, which is actually larger than the one defined in [7]. So the size is basically a scaled-up version. The conference room consisted of tables arranged in u-shaped form. In order to capture the useful components of the channel, the receiver (Rx) must be placed in grid points covering sufficient portions of the room in relation to the transmitter (Tx) locations. A 50λ separation between two Rx locations was used, where λ stands for the wavelength. The basis of this separation is that no change in the average root-mean-square (rms) delay spread with a 25λ separation was found, and the same holds true for 100λ. Details of the room layout and the locations of the Tx and Rx are shown in Figure 1.

Table 2
Candidate Number of Taps N and Their Occurrence Percentage of Greater Than 3%

HPBW pair Candidate $N \rightarrow$	Via-LoS-path scenarios				Via-reflected-path scenarios				
	1	2	3	4	1	2	3	4	5
60° - 60°	84.9	12.7	-	-	61	26.6	4.1	-	-
60° - 30°	91.4	8.1	-	-	67.1	27	4.1	-	-
60° - 15°	6.3	3.7	-	-	35.5	46.9	10.6	5.1	-
30° - 60°	72.1	9	6.7	6.4	50.1	20	14.3	8.6	4.7
30° - 30°	77.5	9.8	10.5	-	62.3	17.9	13.5	5.6	-
30° - 15°	83.4	9.6	7	-	35.6	43.7	15.3	4	-

A 62.5-GHz carrier frequency at 3-GHz bandwidth with 0-dBm power was used for the transmission. Ray tracing simulations were done to capture the channel impulse response. The ray-tracing procedure was developed and verified based on the uniform theory of diffraction. The permittivity and conductivity of concrete, wood, plastic, and glass materials were set to the values applicable for the mmWave region. Since specific antennas were utilized, consequently the mmWave channel that is considered here has the antenna patterns convolved in the impulse responses.

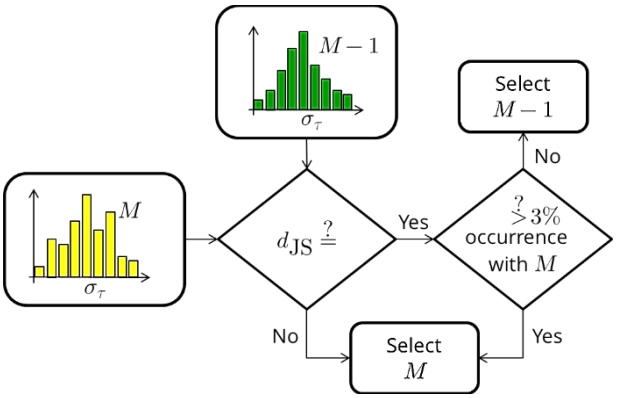

Figure 5: Proposed model order selection process

Two most likely static communication link scenarios were obtained from the simulations: (1) via-LoS-path scenarios and (2) via-reflected-path scenarios. The first scenario considers the LoS path as the communication link between the Tx and Rx antennas, i.e. the Rx points its maximum antenna beam closest to the maximum beam of the Tx. In the second scenario, the link that is considered is through the strongest reflected path or next strongest reflected path. The receiver beams its maximum gain to either arrival direction of these reflected waves. This scenario represents what could happen when the LoS is unavailable, and at least one end of the communications link has antenna beamforming capability in order to direct its main lobe to the desired signal. In order to lessen the complexity of the simulations, directive antennas were used to emulate beamforming. Since the number of antenna element scales proportionally with the beamwidth of

the main lobe, several directive antennas were utilized at the Tx and Rx. The Tx-Rx antenna combinations would result in radio channel models that embed the Tx-Rx antenna attributes with the propagation characteristics. The antennas that were used are reference antennas in IEEE 802.15.3c and IEEE 802.11ad [8]. Figure 2 and Table 1 provide the antenna specifications. So for each link a certain Tx-Rx antenna pair was employed, which are described in terms of their half power beamwidth (HPBW). For example, a 60° - 15° Tx-Rx antenna pair corresponds to the Tx antenna having a main lobe of 60° HPBW, and 15° HPBW for the Rx antenna.

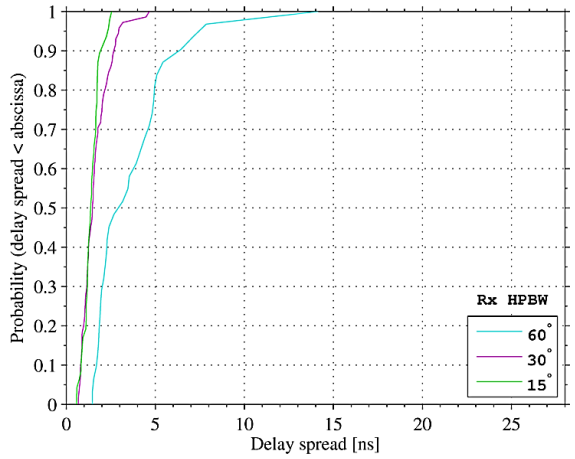

Figure 6: Delay spread distribution in LoS scenarios in which a 30° HPBW Tx antenna was employed

Table 3
Number of Taps Obtained Using the Proposed Model Order Selection Process

Tx-Rx HPBW pair	Via-LoS-path scenario	Via-reflected-path scenario
60° - 60°	3	3
60° - 30°	3	3
60° - 15°	2	6
30° - 60°	5	5
30° - 30°	3	4
30° - 15°	3	4

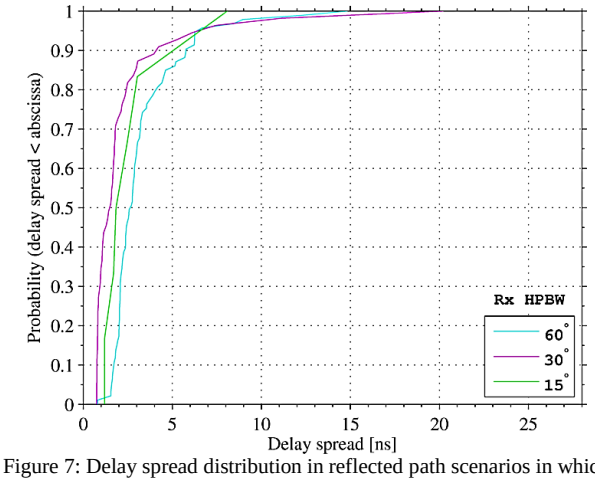

Figure 7: Delay spread distribution in reflected path scenarios in which a 60° HPBW Tx antenna was employed

III. TDL CHANNEL MODEL

The channel impulse responses (CIRs) collected from the simulations were pre-processed before being considered in the model. The time-varying CIR can be expressed in its complex baseband form as a temporal discrete multipath model as follows.

$$h(\tau, t) = \sum_{n} A_n(t)\ \exp\left(\mathrm{j}\phi_n(t)\right)\delta(\tau - \tau_n(t)) \qquad (1)$$

where n is the nth path with amplitude $A_n(t)$, phase shift $\phi_n(t)$, and propagation delay $\tau_n(t)$. $\delta(\cdot)$ denotes the Dirac delta function. A CIR in a specific area is assumed to be generated by the same wide-sense stationary random process, and that each path is an identically distributed random variable and uncorrelated from each other. In the collected CIRs, paths with greater-than-130-dB path loss, 14-m path length, and those below the delay resolution (reciprocal of the bandwidth) were filtered out. The power of the paths was also normalized by the strongest path. This normalization sets the strongest path to 0 dB. Paths with lower than 30-dB-below-the strongest-path were also not considered in the modeling. Such paths do not contribute in achieving high throughput data transfer. Furthermore, the delays were expressed as excess delays relative to the first arriving path. This preprocessing step enables generalization and parameterization of the model. After applying the above mentioned treatment, it was observed that only several paths remained, which are the useful ones for achieving Gbps communications. A consequence of capturing these paths in a model is through a tapped-delay line (TDL) filter shown in Figure 3.

Through the above mentioned preprocessing, a modified TDL channel model is proposed in Figure 4. In the stochastic modeling of the Δ_n power level difference and the τ_n excess delays, individual modeling was performed. Each parameter (Δ_n or τ_n) was modeled per tap, i.e. independently. This per-tap modeling is different from other TDL channel models that models the taps altogether. The novel points then of the proposed TDL channel model are (i) its ability to capture the few useful paths in the mmWave propagation channel that enable Gbps communications using directive antenna patterns, and (ii) each path is individually modeled. Furthermore, since only those paths within 30 dB of the strongest path near the vicinity of the required Rx sensitivity to achieve high throughput are considered, the span then among the taps captures delay spread related effects such as ISI. The difference between each tap takes in the ISI effect. The proposed TDL channel modeling then could basically answer the question of how much percentage in the indoor environment are the delay spread issues prevalent. Knowledge of such occurrence drives which type of equalization will be used in the terminal. Consequently, this leads to low-cost terminals if expensive equalization will not be utilized if the indoor mmWave propagation channel would dictate, since a communication link that have no significant delay spread issue achieves lower bit error rate (BER) than those in severe fading cases. In the following, the parameterization of the proposed TDL channel model is presented.

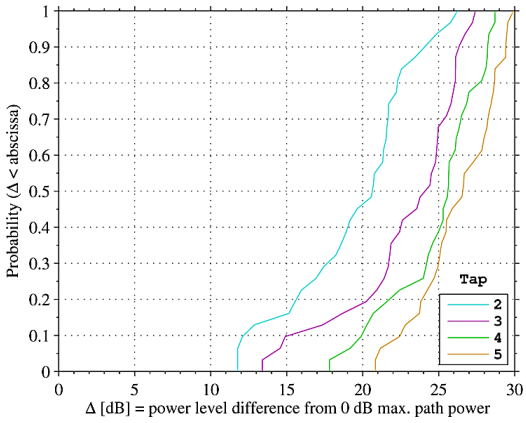

Figure 8: Distribution of the power level difference with N=5 and with the use of a 30°-60° Tx-Rx HPBW pair in via-LoS-path links. It is to be noted that tap 1 has 0 dB level

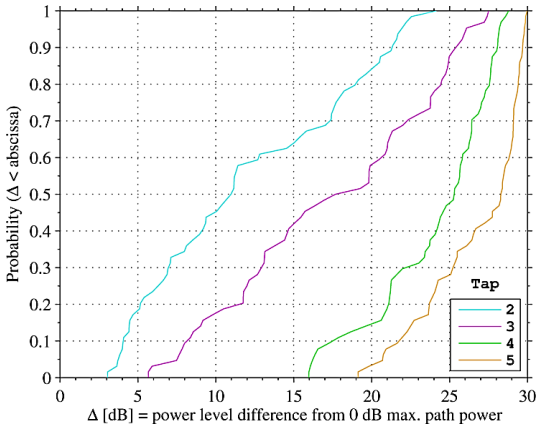

Figure 9: Distribution of the power level difference with N=4 and with the use of a 30°-60° Tx-Rx HPBW pair in via-reflected-path links. Tap 1 has 0 dB level

A. Number of Taps

Table 2 shows the available number of taps N, which is basically the number of paths in the channel. The table also shows how much each N was observed in the conference room. The length of N also indicates the fading in the environment, the longer of which coupled with the depth of each tap reveals delay spread issue scenarios. Thus choosing the appropriate N is crucial. A two-stage process used in this model order selection is proposed. In the first stage, if the probability distributions of the rms delay spread with N=M taps and that with N=M-1 taps are comparably similar, then N=M-1 is pre-chosen. The rms delay spread σ_τ is obtained as

$$\sigma_\tau = \sqrt{\frac{\int_{-\infty}^{\infty} P_h(\tau)\tau^2\,\mathrm{d}\tau}{\int_{-\infty}^{\infty} P_h(\tau)\,\mathrm{d}\tau} - \left(\frac{\int_{-\infty}^{\infty} P_h(\tau)\tau\,\mathrm{d}\tau}{\int_{-\infty}^{\infty} P_h(\tau)\,\mathrm{d}\tau}\right)^2} \qquad (2)$$

where,

$$P_h(\tau) = \int_{-\infty}^{\infty} |h(\tau,t)|^2\,\mathrm{d}\tau \qquad (3)$$

is the delay power spectrum. The second stage only proceeds when N=M-1 is the result of the first stage. In the second stage, M becomes the selected model order if its occurrence percentage is greater than 3%, otherwise the final model order is M-1. If the final model order is M instead of M-1, this means that the occurrence of the significant number of paths is significant to capture the mmWave channel. The similarity was measured by using the Jensen-Shannon divergence d_{JS} between rms delay spread distributions:

$$\begin{aligned} &d_{\mathrm{JS}}\left(\Pr_{(N=M)}, \Pr_{(N=M-1)}\right) \\ &= 0.5 d_{\mathrm{KL}}\left(\Pr_{(N=M)}, \Pr'\right) \\ &+ 0.5 d_{\mathrm{KL}}\left(\Pr_{(N=M-1)}, \Pr'\right) \end{aligned} \qquad (4)$$

where $\Pr_{(N=M)}$ is the probability distribution of the rms delay spread with M ray paths,
$d_{\mathrm{KL}}(\Pr, \Pr'') = \sum_k \Pr(k)\,\log_2[\Pr(k)/\Pr''(k)]$ is the Kullback–Leibler divergence, and
$\Pr' = 0.5(\Pr_{(N=M)} + \Pr_{(N=M-1)})$. Figure 5 depicts this process for model order selection.

Figures 6 and 7 show probability distributions of the rms delay spread from the simulations. The obtained values of the delay spread are also similar to those observed in [9]-[10]. Table 3 shows the achieved number of taps after applying the model order selection process. The results reveal that only several paths are adequate to describe the mmWave propagation channel.

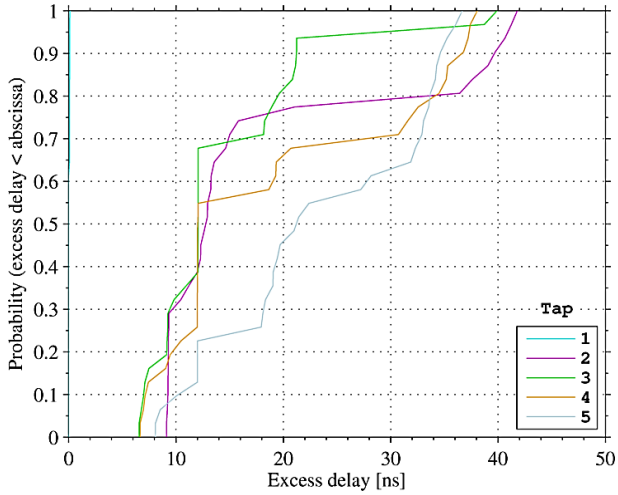

Figure 10: Distribution of the excess delay with N=5 with the use of a 30°-60° Tx-Rx HPBW pair in via-LoS-path links

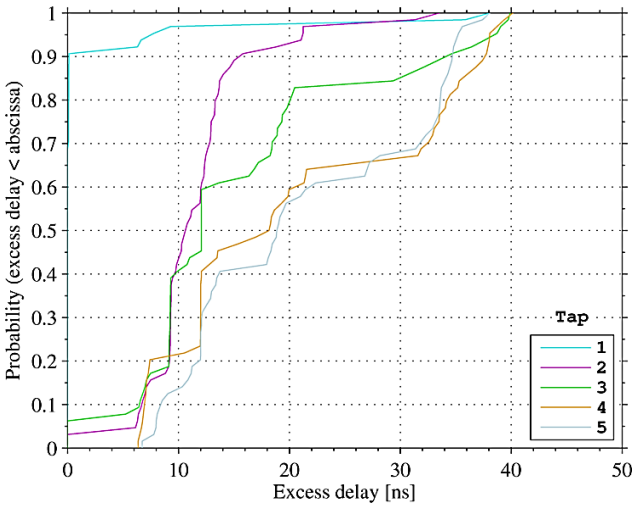

Figure 11: Distribution of the excess delay of with N=5 with the use of a 30°-60° Tx-Rx HPBW pair in via-reflected-path links

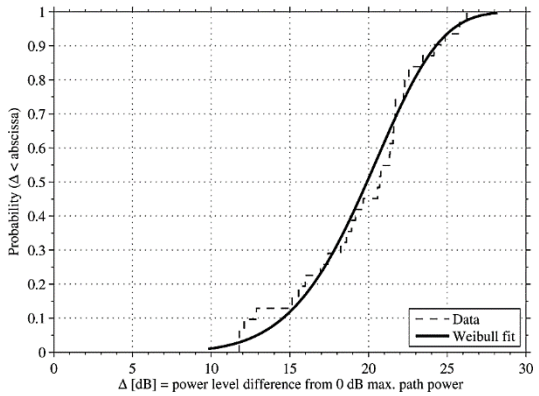

Figure 12: Weibull distribution fitting Δ obtained for 30°-60° Tx-Rx HPBW pair under LoS scenario; β = 21.1492; α = 6.026

Table 4
Best-fit Distribution Parameters of the via-LoS-Path Scenarios

Tx-Rx HPBW pair	Tap	Δ [dB] Weibull (β, α)	τ [ns] Poisson (μ_P)
60° - 60°	1:	-	0
	2:	22.191, 2.5117	9.7441
	3:	29.4685, 50.5646	11.1722
60° - 30°	1:	-	0
	2:	29.6586, 388.8668	12.0615
	3:	29.9312, 409.215	11.9985
60° - 15°	1:	-	0
	2:	25.7492, 4.6238	4.3677
30° - 60°	1:	-	0.0424
	2:	21.1492, 6.026	18.1717
	3:	24.3994, 8.5422	14.5573
	4:	26.1959, 11.2808	19.507
	5:	27.4796, 13.0058	23.7098
30° - 30°	1:	-	0.0663
	2:	24.0283, 4.364	12.1608
	3:	27.4374, 12.8918	16.2424
30° - 15°	1:	-	0.0613
	2:	24.6365, 8.8262	9.6922
	3:	26.0055, 9.7596	10.8481

(-) : defaults to 0-dB level

B. Power Level Difference and Excess Delay

Examples of the probability distributions of Δ_n and τ_n are shown in Figures. 8 to 9, and 10 to 11, respectively. Using the proposed model order selection process in Sec. A to determine N, the statistical parameters of the distribution of Δ_n and τ_n were obtained by maximum likelihood fitting of the collected Δ_n and τ_n CIR data with the finalized probability distribution. The validation of the statistical distribution is discussed in Sec. C. Figure 12 shows an example of the cumulative distribution fit of the power level difference. For via-LoS-path scenarios, the Weibull distribution best fits Δ_n. Its cumulative density function (cdf) is given by.

$$\mathrm{cdf}(\Delta) = 1 - \exp[-(\Delta/\beta)^{\alpha}] \quad (5)$$

where β is the scale parameter, and α is the shape parameter. For via-reflected-path scenarios the exponential distribution best fits Δ_n. Its cdf is given by

$$\mathrm{cdf}(\Delta) = 1 - \exp(-\Delta/\mu_e) \quad (6)$$

where μ_e is the mean. The Poisson distribution was found to best reflect τ_n in order to model the relative arrival times. Its cdf is as follows where μ_P is the mean. Tables 4 and 5 summarize the parameters of the proposed mmWave channel models of the power-delay spectrum, for the via-LoS path and via-reflected waves, respectively.

Table 5
Best-fit Distribution Parameters of the via-Reflected-Path Scenarios

Tx-Rx HPBW pair	Tap	Δ [dB] Exponential (μ_E)	τ[ns] Poisson (μ_P)
60° - 60°	1:	-	3.0824
	2:	13.6395	6.2492
	3:	24.1784	11.3662
60° - 30°	1:	-	4.1036
	2:	19.7856	7.275
	3:	25.0165	11.1408
60° - 15°	1:	-	0
	2:	9.2918	7.6684
	3:	10.7745	6.6315
	4:	23.3428	14.1839
	5:	24.4132	13.7172
	6:	26.2982	8.9396
30° - 60°	1:	-	1.6486
	2:	12.0715	11.6598
	3:	17.5703	15.5622
	4:	24.1687	20.783
	5:	26.8151	21.3245
30° - 30°	1:	-	18.0851
	2:	8.7517	21.6171
	3:	19.8756	15.9771
	4:	27.1999	30.4289
30° - 15°	1:	-	23.1795
	2:	5.3964	24.6196
	3:	17.1587	15.3428
	4:	27.3383	30.5161

Table 6
Hypothesis Testing Outcomes for Δ_n in Via-LoS-Path Scenarios

Hypothesis Test at 5% Significance Level	Candidate distribution		
	Log-normal	Weibull	Exponential
Chi-square goodness-of-fit	Reject	Accept	Reject
Kolmogorov-Smirnov	Reject	Accept	Reject
Jarque-Bera	Reject	t.n.a.	t.n.a.
Lilliefors	Reject	t.n.a.	t.n.a.

t.n.a. : test is not applicable

$$\mathrm{cdf}(\tau) = \exp(-\mu_P) \sum_{k}^{\tau} {\mu_P}^k / k! \quad (7)$$

C. Validation of the Channel Models

The channel models were verified in two ways. For verifying and finalizing the appropriate probability distributions of Δ_n and of τ_n, hypothesis testing was carried out. The parameters of the final distributions were obtained by fitting the obtained data (Δ_n or τ_n) by maximum likelihood estimation. Estimation was done at 95% confidence intervals of the parameters. Outcomes of the hypothesis tests for Δ_n are tabulated in Tables 6 and 7. The results indicate that the Weibull distribution is the best candidate distribution for Δ_n for via-LoS-path scenarios, and the exponential distribution for via-reflected-path scenarios. The hypothesis test results shown in Tables 8 and 9 point that the Poisson distribution for the path arrival times best describes τ_n for both the via-LoS and via-reflected path scenarios.

Aside from the statistical validation of the mmWave TDL channel model parameters and the simulation data by hypothesis testing and maximum likelihood estimation fitting, the mmWave TDL channel models were verified by using external validation. The Shannon channel capacity was used as an external validation metric. Assuming a single-

input-single-output transmission over additive white Gaussian noise and no channel state information at the Tx, the channel capacity C(h) could then be expressed as

$$C(h) = B \log_2\left(1 + \frac{\int_{-\infty}^{\infty} P_h(\tau)\,\mathrm{d}\tau}{P_{\text{noise}}}\right) \quad (8)$$

where B is the signal bandwidth, and P_{noise} is the noise power, wherein same values for each were used in the evaluation. In order to avoid comparing absolute values of C(h), the relative uncertainty ε_ς between the mmWave TDL channel model and the reference CIR data from ray tracing were obtained. It is defined as

$$\varepsilon_\varsigma = \frac{\varsigma(h_{\text{model}})}{\varsigma(h_{\text{reference}})} - 1 \quad (9)$$

where $\varsigma(\cdot)$ is the value produced by the metric, which in this case is C(h). The ideal value of ε_ς is zero, which is perfect correspondence between the model and the reference data. Based on the results (Table 10), it was found that low average values of ε_ς were in the mmWave TDL channel models for via-LoS path scenarios. Values in each scenario indicate that the modeling uncertainty is relatively small.

D. Generating a Channel Impulse Response

The following is a procedure for generating one CIR based on the proposed mmWave TDL channel models.

i. Select the channel scenario and the expected beamwidths of the Tx and Rx antennas, and use Table 4 or Table 5 accordingly.
ii. For each tap, generate Δ_n according to the parameter values and its probability distribution. Do the same for τ_n.
iii. Obtain $A_n(t) = \sqrt{\Delta_n}$ and generate its phase by the uniform probability distribution, i.e. $\phi_n(t) \in [0, 2\pi)$.
iv. Do steps 2 and 3 until all paths have been generated.
v. Obtain the CIR form of the generated mmWave TDL channel model according to (1).

It is to be noted that the time variance in (1) could be obtained by a sequence of CIRs coming from one or different random generator seeds.

IV. CONCLUSION

Channel impulse response models in a conference room indoor environment for millimeter-wave wireless communications are proposed where one end of the communications link has antenna beamforming capability in order to direct its main lobe to the best signal for high-throughput data transfers. The models capture the delay spread issues through the number of taps, power level difference, and excess delay parameters. A criterion for selecting the number of taps is also proposed. It was found that a low number of taps is sufficient for describing the beamformed millimeter-wave propagation channel. Moreover, the proposed tapped-delay line millimeter-wave channel models need to be double-checked with channel sounding or field tests. The results could be used for enhancing the quality of millimeter-wave indoor wireless links.

Table 7
Hypothesis Testing Outcomes for Δ_n In Via-Reflected-Path Scenarios

Hypothesis Test at 5% Significance Level	Candidate distribution		
	Log-normal	Weibull	Exponential
Chi-square goodness-of-fit	Reject	Reject	Accept
Kolmogorov-Smirnov	Reject	Reject	Accept
Jarque-Bera	Reject	t.n.a.	t.n.a.
Lilliefors	Reject	t.n.a.	t.n.a.

Table 8
Hypothesis Testing Outcomes for τ_n in Via-LoS-Path Scenarios

Hypothesis Test at 5% Significance Level	Candidate distribution		
	Poisson	Normal	Exponential
Chi-square goodness-of-fit	Accept	Reject	Reject
Kolmogorov-Smirnov	Accept	Reject	Reject
Jarque-Bera	t.n.a.	Reject	t.n.a.
Lilliefors	t.n.a.	Reject	t.n.a.

Table 9
Hypothesis Testing Outcomes for τ_n in Via-Reflected-Path Scenarios

Hypothesis Test at 5% Significance Level	Candidate distribution		
	Poisson	Normal	Exponential
Chi-square goodness-of-fit	Accept	Reject	Reject
Kolmogorov-Smirnov	Accept	Reject	Reject
Jarque-Bera	t.n.a.	Reject	t.n.a.
Lilliefors	t.n.a.	Reject	t.n.a.

Table 10
Average values of ε_ς [%]

Tx-Rx HPBW pair	Via-LoS-path scenarios	Via-reflected-path scenarios
60° - 60°	-4.35	4.75
60° - 30°	-0.89	4.82
60° - 15°	-0.1	11.32
30° - 60°	-2.66	7.87
30° - 30°	-1.05	12.19
30° - 15°	-0.11	6.95

REFERENCES

[1] Baykas, T., Sum C.-S., Lan Z., Wang J., Rahman M. A., Harada H., and Kato S. 2011. IEEE 802.15.3c: the first IEEE wireless standard for data rates over 1 Gb/s. *IEEE Commun. Mag.* 49:114–121.

[2] IEEE 2012. IEEE Standard Part 11: Wireless LAN Medium Access Control (MAC) and Physical Layer (PHY) Specifications Amendment 3: Enhancements for Very High Throughput in the 60 GHz Band. *IEEE Std 802.11ad-2012.* 1–628.

[3] International Telecommunication Union 2013. *Attenuation by Atmospheric Gases*. *ITU-R P.676-10*

[4] Friis, H. T. 1946. A Note on a Simple Transmission Formula. *Proc. IRE*. 34:254–256.

[5] Maltsev, A. et al. 2010. Channel Models for 60 GHz WLAN Systems. *IEEE 802.11-09/0334r8*.

[6] Yong, S. 2007. TG3c Channel Modeling Sub-committee Final Report. *IEEE 802.15-07-0584-01-003c*.

[7] Perahia, E. et al. 2010. TGad Evaluation Methodology. *IEEE 802.11-09/0296r16*.

[8] Toyoda, I. and Seki, T. 2011. Antenna model and its application to system design in the millimeter-wave Wireless Personal Area Networks standard. *NTT Tech. Rev.* 9: 1–5.

[9] Materum, L., Kato, S. and Sawada H. 2011. Channel Measurements for Short Range Beam Tracking/Switching Systems. *Proc. Int. Symp. Antennas Propagat. (ISAP)*.

[10] Smulders, P. F. M. 2009. Statistical Characterization of 60-GHz Indoor Radio Channels. *IEEE Trans. Antennas Propag*. 57:2820–2829.